Reliability Analysis of Underground Tunnel by A Novel Adaptive Kriging Based Metamodeling Approach

Axay Thapa[a,b], Atin Roy[a], Subrata Chakraborty[a]*

[a]Department of Civil Engineering, Indian Institute of Engineering Science and Technology, Shibpur, India.

[b]Department of Civil Engineering, Sikkim Manipal Institute of Technology, Sikkim Manipal University, Majhitar, India.

*Corresponding Author: Email: schak@civil.iiests.ac.in

Abstract:

An adaptive Kriging based metamodeling approach is explored for tunnel reliability analysis. Specifically, a novel strategy is proposed to select new training points with due consideration to accuracy and efficiency. Based on an initial design of experiments (DOE) following uniform design, an initial Kriging model is constructed. Subsequently, a reduced space is built from the Monte Carlo Simulation (MCS) points located near the limit state surface. Now, the MCS points in close proximity to the existing training points are removed from the reduced space to avoid the clustering effect. Finally, the MCS point having the highest joint probability density value is selected from the reduced space. The inclusion of such point in the DOE is expected to improve the prediction of a maximum number of neighbouring points. Selection of new training points and updating the Kriging model iteratively is continued until no point is left in the reduced space. The estimated failure probability is considered final if its coefficient of variation is less than a predefined threshold. Otherwise, the MCS population is enriched by a new set of MCS samples for further iterations. The effectiveness of the proposed approach is demonstrated by three tunnel reliability analysis problems.

Keywords: Monte Carlo Simulation, Kriging, Adaptive sampling, Joint probability density function, Tunnel reliability.

1. Introduction:

Analysis of tunnel involves immense complexities due to a wide variety of structural and geotechnical parameters [1]. The associated parameters are mostly random in nature [2]. A factor of safety-based deterministic approach is usually applied to consider the effects of uncertainty. However, the approach cannot properly define the tunnel's structural safety level. The reliability analysis is introduced to obtain a rational solution in this regard. Structural reliability analysis (SRA) considers the random variability of structural properties, geotechnical properties, and loads involved in the analysis [3,4]. It provides a visible margin of safety by considering the statistical distribution of the variables in the analysis which a deterministic analysis fails to yield.

The application of SRA is enormous [5–10]. The primary task is to obtain the probability of failure of a structure which requires evaluating a multidimensional integral involving the joint probability distribution function (PDF) of the input random parameters. However, analytical integration is a difficult task, and various approximations are made to estimate the reliability. The analytical method of approximation includes the first-order reliability method (FORM) [11] and the second-order reliability method (SORM) [12], which involves the Taylor series expansion of the associated LSF [13]. Alternatively, the Monte Carlo simulation (MCS) based reliability analysis method is the most accurate and straightforward approach. However, the technique requires several simulations involving repetitive evaluations of a limit state function (LSF). Thus, huge computation time is required by the MCS technique for estimating the reliability of a structure. Especially when a Finite Element (FE) analysis is involved in obtaining the value of the related implicit LSF. In this regard, the metamodeling technique has emerged as an effective alternative. A metamodel represents the implicit LSF with an explicit form to eliminate the complexities and time-consuming, repetitive FE analyses. The reliability analysis aided with metamodel has been widely applied in engineering problems [5]. Various metamodels have been developed e.g., the usual polynomial response surface method (RSM) [14,15], the moving least square method (MLSM) [16], the support vector machine (SVM) classification [17,18], the support vector regression (SVR) [8,19,20], the radial basis function networks (RBFN) [9], the Kriging method [7], the artificial neural networks (ANN) [21], etc. The samples carefully selected for metamodel training are known as the design of experiment (DOE). The accuracy and efficiency of a metamodel largely depend on the sampling approach and the number of training samples. In metamodel based SRA, the metamodel requires better prediction accuracy near the limit state surface for estimating reliability efficiently. However, the limit state surface being implicit in nature is not known a priori. Various sampling strategies are proposed to circumvent the difficulty. One such concept is the reconstruction of an initial DOE iteratively [6,19,22–24]. However, such an approach does not use the previous DOE data. Thereby, results in the wastage of valuable data obtained by intensive computational techniques. Adaptive sampling sequentially is an emerging concept that augments the DOE by adding new training samples iteratively [25–30]. The adaptive Kriging combined with MCS (AK-MCS) method developed by Echard et al. [26] based on the active learning approach where one new training sampling is selected by a learning function per iteration until the corresponding stopping condition is met. Active learning-based adaptive Kriging methods are widely applied in the field of SRA [27,31–35]. Successful applications of the sequential adaptive sampling approach for SRA using other metamodels like MLSM [36], SVM classification [28], SVR [37,38] etc. are also noted.

Tunnel reliability analysis has also gained momentum over the past few decades. Hoek [1] performed the reliability analysis of a tunnel by applying the MCS approach. Oreste [39] presented a probabilistic numerical approach for the design of primary tunnel support by the hyper-static reaction method. They employed the MCS technique considering the probabilistic distributions of the geo-mechanical index of the rock mass and the mechanical parameters of the support material. Li and Low [40] implemented the FORM and MCS approach to assess the reliability of a circular tunnel under a hydrostatic stress field. Chen et al. [41] performed the reliability analysis of a real-life tunnel, based on the FORM. Apart from these, various metamodel based approaches have also been applied for tunnel reliability analysis. Mollon et al. [42] presented a usual polynomial RSM based reliability analysis of a shallow circular tunnel driven by a pressurized shield in soil defined by the Mohr-Coulomb failure criterion. Other successful applications of the RSM based metamodel in assessing tunnel reliability can also be noted [43,44]. Zhang and Goh [45] developed an approach for tunnel reliability analysis using a neural network-based metamodel. Lü et al. [46] performed a probabilistic ground-support interaction analysis of a deep rock excavation using an ANN and uniform design (UD) based on the convergence–confinement method. Liu and Low [47] proposed a modified hybrid approach by combining RSM and ANN to assess the system reliability of rock-tunnel with rock bolts. The SVM [48], Kriging (Yonghua et al. 2009), and RBFN [49,50] based metamodels have also been successfully implemented in the reliability analysis of tunnels. Hybrid techniques were also attempted for tunnel reliability analysis by combining two or more metamodels [51,52]. It is noted that most of the existing studies on metamodel based tunnel reliability analysis construct the DOE by one-shot sampling. However, the application of the adaptive sampling-based approach for tunnel reliability analysis is noted to be very limited. For example, Wang and Fang [50] developed an adaptive RBFN for the reliability analysis of tunnels. The study is limited to the FORM-based approach. Li and Yang [53] proposed an adaptive Kriging based approach for tunnel reliability analysis. To select the adaptive training points near the failure plane, a bisection search was employed. The method demands around 200-250 function evaluations which are even higher than that required by the AK-MCS [26] and the adaptive SVM [28] methods. Thus, further study on the adaptive sampling-based metamodeling approach for sufficient accurate and efficient tunnel reliability analysis seems to be important.

In the present study, an adaptive Kriging based metamodeling approach is explored for tunnel reliability analysis. Specifically, a novel strategy is proposed to select new training points with due consideration to accuracy and efficiency. It can be noted that the minimum number of training samples required to build a Kriging model is independent of the problem dimensionality. Thus, following Echard et al. [26], the number of training samples in the initial DOE is taken as 12. However, for better approximation from the starting of the adaptive approach, the initial DOE is constructed by the UD method, instead of randomly selecting from the MCS points [26]. For this, a reduced space is constructed first from the MCS points located near the limit state surface to select the next training point. Then, the MCS points in close proximity to the existing training points are removed from the reduced space to avoid the clustering effect. Finally, the MCS point having the highest joint PDF value is selected from the reduced space. The inclusion of this point in the DOE is expected to improve the prediction of a maximum number of neighbouring points. Selection of a new training point and updating the Kriging model iteratively is continued until no point is left in the reduced space. The estimated failure probability is considered final if its coefficient of variation (COV) is less than a predefined threshold, otherwise, the MCS population is enriched by a new set of MCS samples for further iterations. The proposed adaptive Kriging method is illustrated by considering three tunnel reliability analysis problems. The efficiency and accuracy of the proposed method are compared with the AK-MCS method, considering the results of the direct MCS technique as the benchmark.

2. Reliability analysis of Tunnel by adaptive metamodeling approach

The proposed adaptive metamodeling approach of tunnel reliability analysis is hinged on Kriging based metamodel. Thus, a brief theoretical background of Kriging based metamodel is provided first. Then, the proposed adaptive Kriging approach is presented.

2.1 Kriging based Metamodel

The Kriging model combines a regression function and a Gaussian stochastic process [54]. The regression part provides the global trend, and the stochastic part shapes the local trend of the model. For a *n*-dimensional input variable, **x**, the Kriging model can be represented as,

$$g(\mathbf{x}) = \mathbf{f}(\mathbf{x})^{\mathrm{T}}\boldsymbol{\beta} + Z(\mathbf{x}) \tag{1}$$

where, $\mathbf{f} = [f_{1,\ldots}, f_k]$ is a set of *k* known functions and $\boldsymbol{\beta} = [\beta_1, \ldots, \beta_k]^{\mathrm{T}}$ is the corresponding regression coefficient vector. $Z(\mathbf{x})$ is a stationary Gaussian process with zero mean and covariance between two points **x** and **w**, $Cov[Z(\mathbf{x}), Z(\mathbf{w})] = \sigma_Z^2 R_\theta(\mathbf{x}, \mathbf{w})$; where, σ_Z^2 is the process variance and R_θ is the correlation function. There is a variety of functional forms defining the correlation. The following anisotropic Gaussian correlation model is considered in the present study,

$$R_\theta(\mathbf{x}, \mathbf{w}) = \prod_{i=1}^{n} \exp\left(-\theta_i \left|x_i - w_i\right|^2\right) \tag{2}$$

x_i and w_i are the i^{th} coordinate point of **x** and **w.**

For a given *p* number of training samples $\mathbf{S} = [\mathbf{S}_{1,\ldots}, \mathbf{S}_p]^{\mathrm{T}}$ and corresponding actual output $\mathbf{g} = [g_1, \cdots, g_p]^{\mathrm{T}}$, the values of $\boldsymbol{\beta}$ and σ^2 can be estimated as [55],

$$\hat{\boldsymbol{\beta}} = \left(\mathbf{F}^T\mathbf{R}^{-1}\mathbf{F}\right)^{-1}\mathbf{F}^T\mathbf{R}^{-1}\mathbf{g} \tag{3}$$

$$\hat{\sigma}^2 = \frac{1}{p}(\mathbf{g} - \mathbf{F}\hat{\boldsymbol{\beta}})^T\mathbf{R}^{-1}(\mathbf{g} - \mathbf{F}\hat{\boldsymbol{\beta}}) \tag{4}$$

where, $\mathbf{R} = \left\{R_\theta\left(\mathbf{x}_i, \mathbf{x}_j\right)\right\}_{1\le i,j\le p}$ is the correlation matrix of dimension (p×p) and $\mathbf{F} = \left[\mathbf{f}\left(\mathbf{S}_1\right), \cdots, \mathbf{f}\left(\mathbf{S}_p\right)\right]^{\mathrm{T}}$ is the design matrix of dimension (p×k). The values of $\hat{\beta}$ and $\hat{\sigma}^2$ are dependent on the value of θ. Thus, θ is first obtained by minimising the maximum likelihood estimation, $\Psi(\theta) = \left|R(\theta)\right|^{\frac{1}{p}}\sigma(\theta)^2$. The achieved predictor $g(x)$ with parameters: $\beta = \hat{\beta}$; $\sigma^2 = \hat{\sigma}^2$ and $\theta = \widehat{\theta}$; is known as the maximum likelihood empirical 'best linear unbiased predictor' (BLUP), and is evaluated by,

$$g(\mathbf{x}) = \mathbf{f}(\mathbf{x})^{\mathrm{T}}\hat{\beta} + \mathbf{r}(\mathbf{x})^{\mathrm{T}}\mathbf{R}^{-1}(\mathbf{g} - \mathbf{F}\beta) \tag{5}$$

where, $\mathbf{r}(\mathbf{x}) = \left[R_\theta(\mathbf{x},\mathbf{S}_1),\cdots,R_\theta(\mathbf{x},\mathbf{S}_p)\right]^T$. The Kriging variance $\sigma_G^2(\mathbf{x})$ as is given by,

$$\sigma_G^2(\mathbf{x}) = {\sigma_z}^2\left[1 + \mathbf{u}(\mathbf{x})^T(\mathbf{F}^T\mathbf{R}^T\mathbf{F})^{-1}\mathbf{u}(\mathbf{x}) - \mathbf{r}(\mathbf{x})^T\mathbf{R}^{-1}\mathbf{r}(\mathbf{x})\right], \tag{6}$$

where, $\mathbf{u}(\mathbf{x}) = \mathbf{F}^T\mathbf{R}^{-1}\mathbf{r}(\mathbf{x}) - \mathbf{f}(\mathbf{x})$.

2.2 Proposed adaptive Kriging based metamodeling approach for reliability analysis

The proposed approach of tunnel reliability analysis is basically an adaptive Kriging based metamodeling approach in the framework of MCS technique. It is well known that the accuracy of metamodel in estimating probability of failure directly depends on the correct sign prediction at the MCS points. In order to achieve this, an adaptive sampling-based metamodeling approach is proposed here. The approach starts with an initial DOE to build an initial Kriging model. Then, a new training point, based on the prediction of the previous Kriging model along with certain selection criteria, is added to the existing DOE. Subsequently, the Kriging model is updated with the enriched DOE. This updating process is continued iteratively until a stopping condition is satisfied. The proposed adaptive approach is presented in detail in the following sections.

2.2.1 Initial DOE

A good initial DOE can provide an initial metamodel with better accuracy and can efficiently select adaptive training samples for further improvement. However, the number of training points in the initial DOE will be restricted to ensure computational efficiency. Thus, a good sampling scheme should be adopted to build the initial DOE. In reliability analysis problems involving implicit LSF, the position of the limit state surface is not known a priori. Based on the assumption that the limit state surface is equally likely to be located anywhere in the input space, an initial DOE should construct metamodel using samples distributed as uniform as possible over the entire input space. This can be achieved by a space-filling design suitable for computer experiments where replication error is absent, unlike the physical experiments. The uniform design (UD) and Latin hypercube designs are the two most popularly used space-filling designs [56]. However, among all the space-filling designs, UD [57] has the lowest discrepancy. Therefore, UD is chosen to construct the initial DOE. The initial sample size is taken as 12 following Echard et al. [26] for all the cases since the minimum number of training points required by ordinary Kriging is independent of the input dimension of the problem.

2.2.2 Adaptive scheme for DOE enrichment

To improve the accuracy of estimated failure probability, the training of the metamodel should approximate a LSF with sufficient accuracy so that the approximated LSF at any simulation point could predict the correct sign of the LSF. In the proposed adaptive scheme, the DOE is enriched by sequentially adding new training samples to enhance the response approximation capability of the metamodel towards getting the accurate sign. For this, the new training points are selected close to the limit state surface where the chance of misrecognition of sign is very high. At the same time, the point must not be in very close proximity to the existing training samples to prevent data clustering and wastage of data. Nevertheless, the new training point should have a value of joint PDF as high as possible. This is expected to improve the prediction at a maximum number of MCS points. In this regard, it can be noted that the density of MCS points is high where the value of the joint PDF is high. Thus, the inclusion of a point having a high joint PDF value in the DOE is expected to improve the prediction of a large number of MCS points in its neighbourhood. The updating of the DOE is made by adding new training samples adaptively by satisfying the above-mentioned two criteria simultaneously. This will involve the solution of a multi-criterion optimization problem. A simple optimization procedure is attempted here by defining a constrained optimization problem where the joint PDF is to be maximized with two constrains. One is based on the minimum distance from the existing training samples to avoid data clustering and the other one is based on the maximum magnitude of the approximated LSF to ensure the closeness to the limit-state surface. The optimization problem can be expressed as follows,

$$\begin{aligned} &\text{Max.} \quad F_X\left(\mathbf{X}^*\right) \\ &\text{s. t.} \quad \begin{cases} \left|\hat{g}\left(\mathbf{X}^*\right)\right| \le y_{thr} \\ \min\left\{\left\|\mathbf{x}^* - \mathbf{s}_1\right\|, \cdots, \left\|\mathbf{x}^* - \mathbf{s}_p\right\|\right\} \ge d_{thr} \end{cases} \end{aligned} \tag{1}$$

where, $F_X\left(\mathbf{X}^*\right)$ and $\left|\hat{g}\left(\mathbf{X}^*\right)\right|$ are, respectively the value of the joint PDF and the magnitude of the approximated LSF, $\hat{g}$ at the next best point, $\mathbf{X}^*$; y_{thr} is considered as the maximum magnitude of the LSF that can be allowed at the point and $\|\ \|$ denotes the Euclidian norm which is used for measuring the distance between two points. Before measuring the Euclidian distances, the original input space is scaled down to a standardised space where each variable has zero mean and unit SD. Thereby, $\mathbf{x}^*$ is the point in the standardised space corresponding to the point $\mathbf{X}^*$ in the original input space. Similarly, $\mathbf{s}_1,\cdots,\mathbf{s}_p$ are the points in the standardised space corresponding to the *p* training points of the existing DOE. Here, d_{thr} is considered as the minimum Euclidian distance in the standardised space by which the new training point is separated from any existing training point. The optimization problem described in Eq. (1) is further simplified by restricting the searching within the MCS population only, instead of the whole input domain. Finally, a reduced space is obtained from the MCS population by excluding the points which do not satisfy the two constraints described by Eq. (1). This is the final search domain to obtain the next best training point.

In the present study, the value of d_{thr} is taken as 0.5 unit which implies the minimum distance between any two training points is half of the SD in the standardised input space. The value of y_{thr} is decided from the CDF of the approximated response based on the estimated failure probability and its COV. This is simply taken as the magnitude of the response for which its CDF value is equal to (1-COV) times the estimated P_f. Mathematically, it can be expressed as follows,

$$y_{thr} = \left|F_{\hat{g}}^{-1}\left(\hat{P}_f - \delta_{\hat{P}_f}\hat{P}_f\right)\right| \tag{2}$$

where, $F_{\hat{g}}^{-1}$ represents the inverse CDF of $\hat{g}$, the LSF approximated by the Kriging model, $\hat{P}_f$ is the value of P_f estimated by the Kriging model and $\delta_{\hat{P}_f}$ is its COV computed as follow,

$$\delta_{\hat{P}_f} = \sqrt{\frac{1-\hat{P}_f}{\hat{P}_f N_{MC}}} \tag{3}$$

The maximum allowable value of $\delta_{\hat{P}_f}$ is taken as 5% for an efficient MCS study.

2.2.3 Outline of the proposed adaptive Kriging approach

An initial DOE consisting of 12 samples (as described in sec 2.2.1) is prepared first by UD within the physical domain of the random variables. Then, based on the initial DOE, the Kriging model is constructed. The DACE MATLAB toolbox [58] is used for this. In estimating the failure probability by the MCS, N_{MCS} samples for each random variable are generated from the respective probability distribution. The value of the joint PDF at each MCS point is determined. Then, based on the Kriging model, the LSF is approximated at all the MCS points to estimate the $\hat{P}_f$ value and $\delta_{\hat{P}_f}$. Now, a reduced space is constructed for selecting the new training point. This is done by building a set of MCS points having magnitude of approximated LSF less than y_{thr} and then excluding the MCS points those are located within a distance of 0.5 unit from the nearest training point in the standardised input space. Now, the point having the highest joint PDF in the present reduced space, (i.e., after the exclusion) is selected as the next best training sample.

The actual LSF is evaluated at the selected point to add it to the DOE. The Kriging model is updated with the augmented DOE. In this way, the adaptive sampling process is continued iteratively. If there is no point left in the reduced space and $\delta_{\hat{P}_f}$ is below 5%, then, the adaptive iteration is stopped. On the other hand, if the reduced space is empty, but, $\delta_{\hat{P}_f}$ is found to be high (>5%), the MCS population is enriched by adding newly generated N_{MC2} numbers of MCS. The entire process is depicted by a flowchart in Fig. 1.

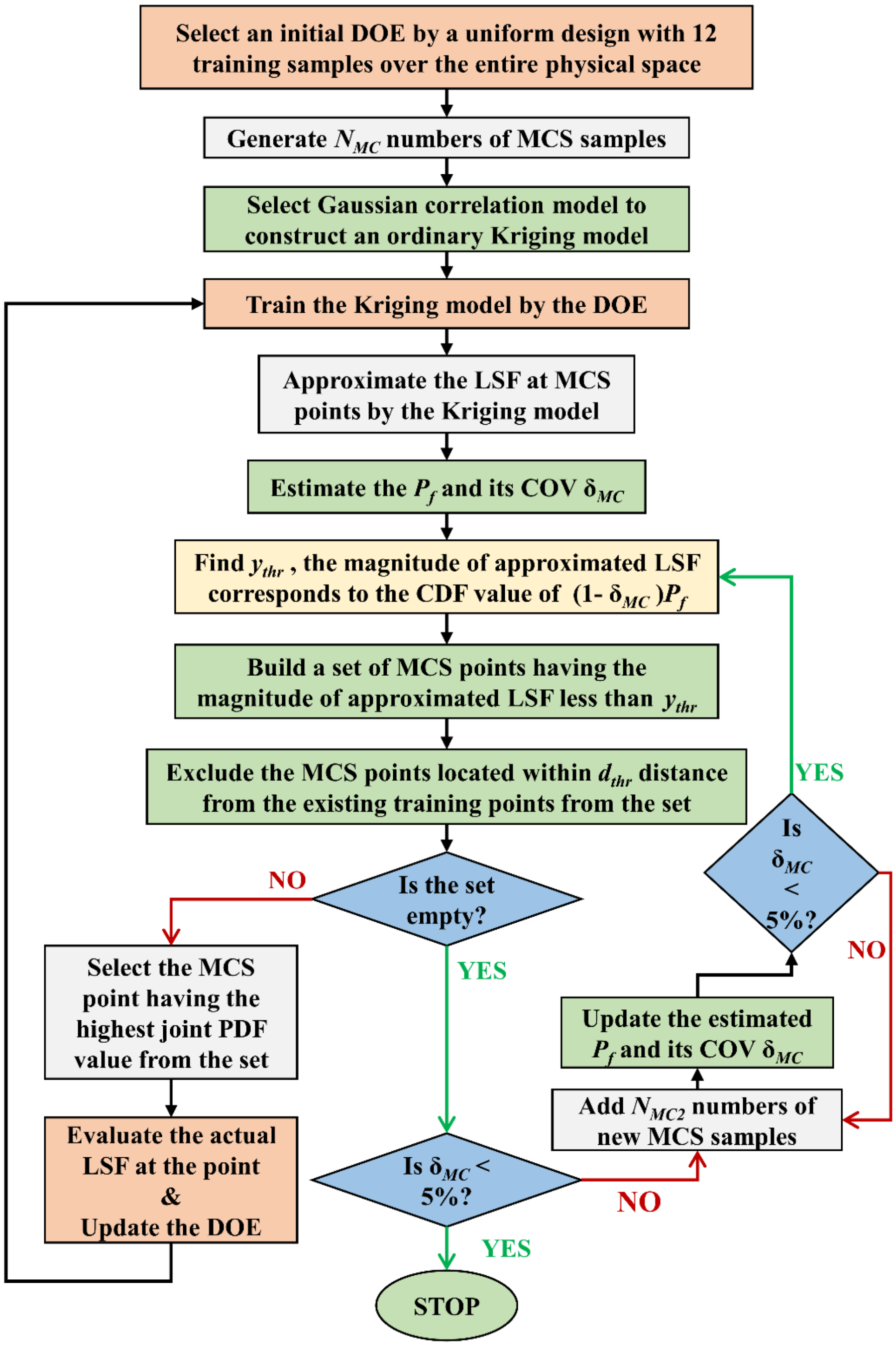

Fig. 1. Flowchart of the proposed adaptive Kriging method.

3. Numerical Study

The effectiveness of the proposed adaptive Kriging approach for reliability analysis of tunnel is elucidated by considering three examples. The first one is a circular tunnel subjected to hydrostatic insitu stress, where explicit analytical form of the LSFs are readily available. The second example is a real-life tunnel (Liziping Tunnel, China) in which the involved LSF has an analytical form but implicit in nature. In the last example, the LSF of a deep circular tunnel with concrete liner and rockbolt is required to be obtained by FE analysis considering more realistic geostatic stress condition. In the proposed adaptive Kriging approach, 12 number of samples are constructed according to an appropriate UD table readily available at: https://www.math.hkbu.edu.hk/UniformDesign/. For comparative study, the failure probabilities are also estimated by the AK-MCS method [26]. In doing so, the U function proposed by Echard et al. [26] is employed as the learning function. The accuracy is judged by comparing with the results of direct MCS technique.

3.1 Example 1: a circular tunnel with hydrostatic insitu stress

A circular tunnel subjected to a far-field hydrostatic stress $\boldsymbol{p_o}$ and an applied internal stress $\boldsymbol{p_i}$, having an internal radius of $\boldsymbol{R_t}$ and an effective plastic zone radius R_p as shown in Fig. 2 is considered. The tunnel is subjected to far-field hydrostatic stress, p_o and applied internal stress, p_i. The Mohr-Coulomb failure criterion is used to define the elastoplastic behaviour of the rock mass. Based on the plain strain formulation of the tunnel in a rock mass, the radius of plastic zone and radial displacement are [59]:

$$R_p = R_t \left(\frac{2(p_o.\sin\varphi + c.\cos\varphi)}{2p_i.\sin\varphi + c.\cos\varphi} \right)^{\frac{1-\sin\varphi}{2\sin\varphi}} \tag{4}$$

$$u_{rp} = \frac{R_t(1+\nu)}{E_r} \left[(2p_o \sin\varphi(1-\nu) - c.\cos\varphi) \left(\frac{R_p}{R_t} \right)^2 - (1-2\nu)(p_o - p_i) \right] \tag{5}$$

where, $\boldsymbol{E_r}$ and $\boldsymbol{\nu}$ are the deformation modulus and Poisson's ratio of the rock mass, respectively.

The cohesion, elastic modulus, angle of internal friction and the Poisson ratio of the rock mass are used to define the elastoplastic behaviour of the tunnel. The Poisson's ratio of the rockmass is taken as 0.22. The statistical properties of the parameters which are considered random are shown in Table 1.

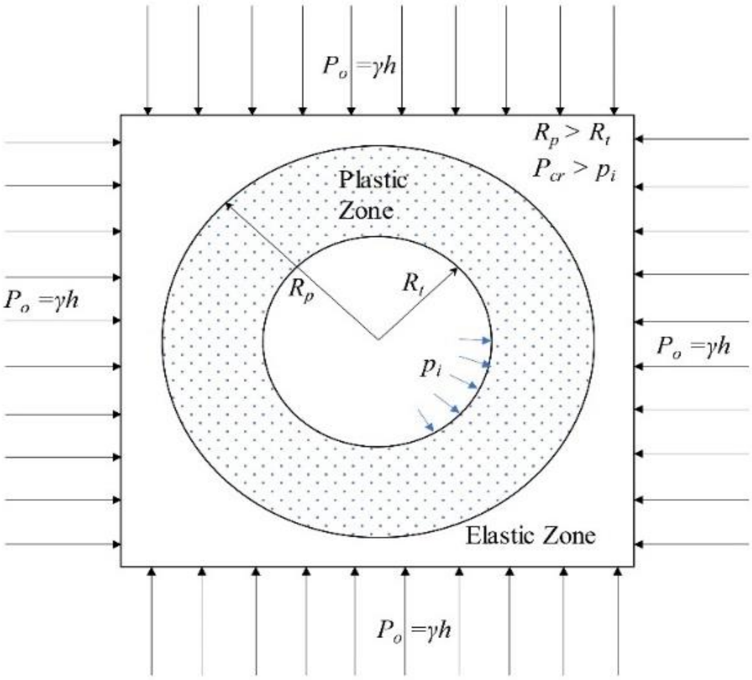

Fig. 2. A circular deep tunnel subjected to hydrostatic stress with internal pressure less than the critical pressure

Table 1 Statistical properties of the variables for Example 1 [43]

Random variables	Unit	Distribution	Mean	SD	Truncation Limit	
					Lower	Upper
Elastic Modulus (E)	MPa	Truncated Normal	1185	330	195	2175
Cohesion (c)	MPa	Truncated Normal	0.28	0.06	0.1	0.46
The angle of internal friction (φ)	Degree	Truncated Normal	23.7	3.4	13.5	33.9

The reliability analysis of the tunnel is performed with respect to the allowable plastic radius and radial displacement of the tunnel wall. The associated two LSFs can be expressed as,

$$g_1(x) = \lambda - \frac{R_p}{R_t} \tag{6}$$

$$g_2(x) = \varepsilon - \frac{u_{rp}}{R_t} \tag{7}$$

In Eq. (6), the performance threshold λ is the allowable value of the ratio between the plastic zone radius and the radius of the tunnel. It depends directly on the maximum size of the plastic zone which is in the tunnel face derived by applying the least internal stress i.e., nil. The value of ε in Eq. (7) is the ratio of the maximum radial displacement of the tunnel wall and the radius of the tunnel. Unless mentioned otherwise, the values of λ and ε are taken as 3 and 2%, respectively [40,48,50,60].

The initial DOE is constructed according to the UD table $U_{12}(12^2)$ and the tunnel reliability is estimated accordingly by the proposed approach as outlined in subsection 2.2.3. Further, the failure probability is also estimated by the AK-MCS method [26] for comparative study. The results obtained by the direct MCS method are considered as the benchmark for the comparison. Initially, N_{MC} = 100000 is considered. The COV of P_f is evaluated once the stopping condition is satisfied. If the value is higher than 5%, then further 50000 MCS samples are added to N_{MC}. The iteration is continued till the value of COV of P_f becomes less than 5%. The estimated P_f, value and its COV, the number of actual function evaluation (N_E), and the number of simulations, N_{MC} by the proposed adaptive Kriging, the AK-MCS and the direct MCS methods for LSF $g_1(x)$ for varying p_o (p_i = 1.05 N/mm^2; λ = 3), varying p_i (p_o = 5 N/mm^2; λ = 3) and varying λ (p_o = 5 N/mm^2; p_i= 1.05 N/mm^2) are compared in Table 2, 3 and 4, respectively. The result of the comparative study shows that the reliability results are in very close agreement with the results obtained by the direct MCS technique. However, the samples required by the proposed method is either equal or less than the samples required by the AK-MCS method in most of the cases.

Table 2. Comparison of probability of failure P_f values for LSF $g_1(x)$ for varying p_o (p_i = 1.05 N/mm^2; λ = 3)

p_o (N/mm^2)	Direct MCS		AK-MCS		Proposed Adaptive Kriging	
	P_f (N_E)	N_{MC} (COV of P_f)	P_f (N_E)	N_{MC} (COV of P_f)	P_f (N_E)	N_{MC} (COV of P_f)
4.5	0.00134 (4×10^5)	4×10^5 (4.3%)	0.00133 (12+10)	3.5×10^5 (4.98%)	0.00134 (12+2)	3.5×10^5 (4.63%)
4.75	0.00268 (2×10^5)	2×10^5 (4.3%)	0.00272 (12+8)	1.5×10^5 (4.94%)	0.00273 (12+4)	1.5×10^5 (4.94%)
5	0.00539 (1×10^5)	1×10^5 (4.3%)	0.00539 (12+12)	1×10^5 (4.29%)	0.00539 (12+12)	1×10^5 (4.30%)
5.25	0.00888 (1×10^5)	1×10^5 (3.3%)	0.00888 (12+8)	1×10^5 (3.34%)	0.00891 (12+7)	1×10^5 (3.34%)
5.5	0.01374 (1×10^5)	1×10^5 (2.7%)	0.01374 (12+9)	1×10^5 (2.68%)	0.01374 (12+9)	1×10^5 (2.68%)

Table 3. Comparison of probability of failure P_f values for LSF $g_1(x)$ for varying p_i and (p_o = 5 N/mm^2; λ = 3)

p_i (N/mm^2)	Direct MCS		AK-MCS		Proposed Adaptive Kriging	
	P_f (N_E)	N_{MC} (COVof P_f)	P_f (N_E)	N_{MC} (COVof P_f)	P_f (N_E)	N_{MC} (COVof P_f)
0.75	0.03373 (1×10^5)	1×10^5 (1.7%)	0.03373 (12+8)	1×10^5 (1.69%)	0.03376 (12+8)	1×10^5 (1.69%)
0.9	0.01388 (1×10^5)	1×10^5 (2.7%)	0.01388 (12+11)	1×10^5 (2.67%)	0.01391 (12+9)	1×10^5 (2.66%)
1.05	0.00539 (1×10^5)	1×10^5 (4.3%)	0.00539 (12+12)	1×10^5 (4.30%)	0.00539 (12+12)	1×10^5 (4.29%)
1.2	0.00164 (3×10^5)	3×10^5 (4.5%)	0.00164 (12+10)	$2.\ \times10^5$ (4.88%)	0.00169 (12+3)	2.5×10^5 (4.86%)
1.35	0.00034 (2×10^6)	2×10^6 (3.8%)	0.00034 (12+10)	1.2×10^6 (0.24%)	0.00035 (12+4)	1.2×10^6 (5%)

Table 4. Comparison of probability of failure P_f values for LSF $g_1(x)$ for varying λ and (p_o = 5 N/mm^2; p_i= 1.05 N/mm^2)

λ	Direct MCS		AK-MCS		Proposed Adaptive Kriging	
	P_f (N_E)	N_{MC} (COVof P_f)	P_f (N_E)	N_{MC} (COVof P_f)	P_f (N_E)	N_{MC} (COVof P_f)
2.5	0.02758 (1×10^5)	1×10^5 (1.9%)	0.02759 (12+8)	1×10^5 (1.88%)	0.02760 (12+8)	1×10^5 (1.88%)
2.75	0.01185 (1×10^5)	1×10^5 (2.9%)	0.01185 (12+8)	1×10^5 (2.89%)	0.01185 (12+8)	1×10^5 (2.89%)
3	0.00539 (1×10^5)	1×10^5 (4.3%)	0.00539 (12+12)	1×10^5 (4.30%)	0.00539 (12+12)	1×10^5 (4.29%)
3.25	0.00221 (2.5×10^5)	2.5×10^5 (4.3%)	0.00212 (12+10)	2×10^5 (4.86%)	0.00214 (12+4)	2×10^5 (4.83%)
3.5	0.00103 (5×10^5	5×10^5 (4.4%)	0.00105 (12+12)	4×10^5 (4.87%)	0.00106 (12+4)	4×10^5 (4.87%)

Further, the absolute percentage errors in estimating P_f values by the proposed adaptive Kriging and the AK-MCS methods for the first LSF $g_1(x)$ for varying p_o, p_i and λ are shown in Fig. 3 to readily compare the accuracy. The proposed adaptive Kriging approach is observed to be quite accurate.

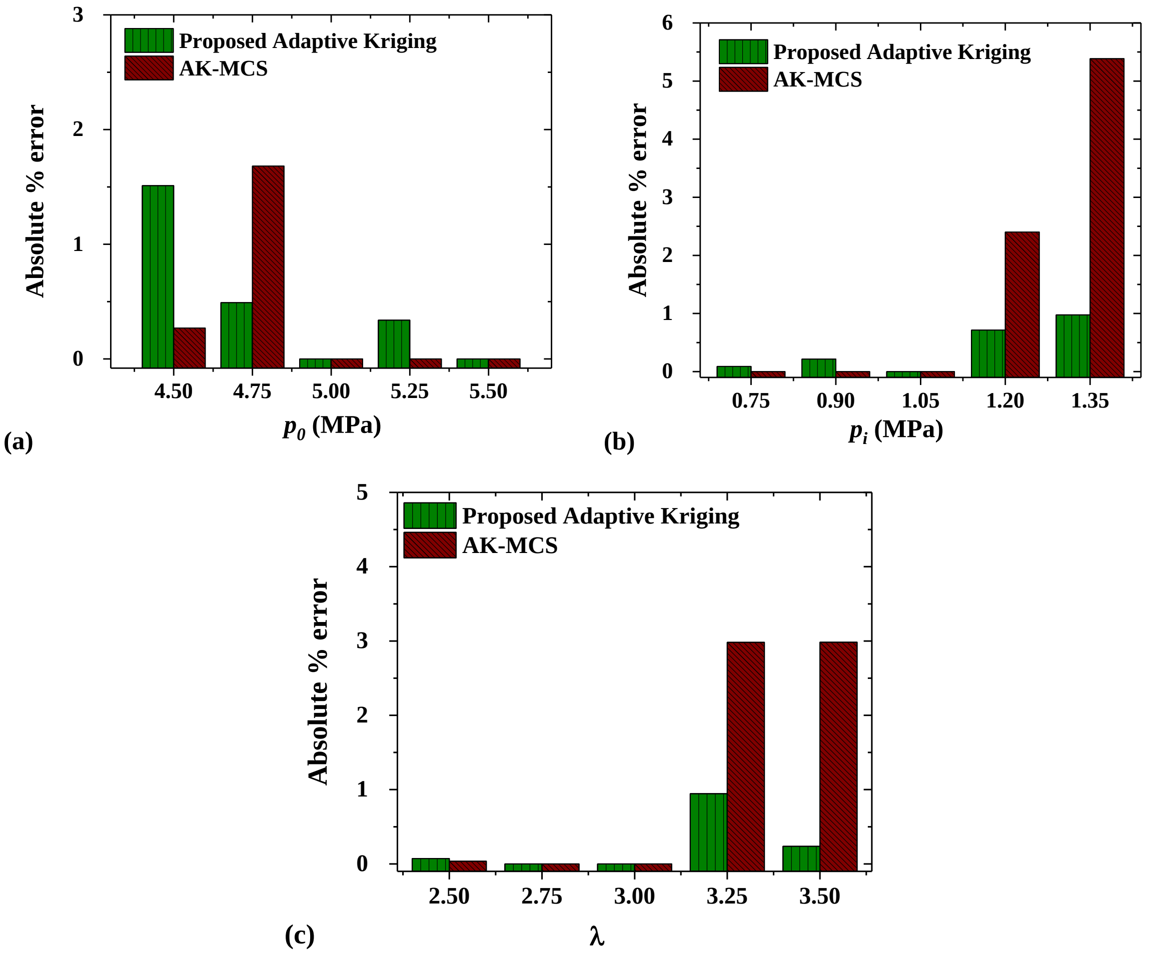

Fig. 3. Comparison of absolute percentage errors in estimating P_f values by the proposed adaptive Kriging and the AK-MCS methods for the first LSF.

Now, the sensitivity study of the proposed approach with respect to DOE data is performed by varying the initial DOE size. For p_o = 5 N/mm^2, p_i = 1.05 N/mm^2 and λ = 3, the P_f values are estimated by the proposed method for four different initials DOEs according to UD tables $U_{12}(12^2)$, $U_{18}(18^2)$, $U_{24}(24^2)$ and U_{30} (30^2). The total number of training sample required, and the number of adaptive samples added by the proposed method for different size of initial DOE are shown in Fig. 4 (a) for the first LSF. Fig. 4 (b) shows the absolute percentage error in estimating the failure probability for the four different cases and noted to be very low. As expected, the number of adaptive samples are decreasing with the increasing number of initial training samples. Though the number of adaptive samples added is reduced, the total number training sample is increasing with the initial DOE size. Therefore, 12 number of initial samples seems to be a balance choice as accuracy level is found to be very high. The results of the sensitivity study clearly reveal the robustness of the proposed approach.

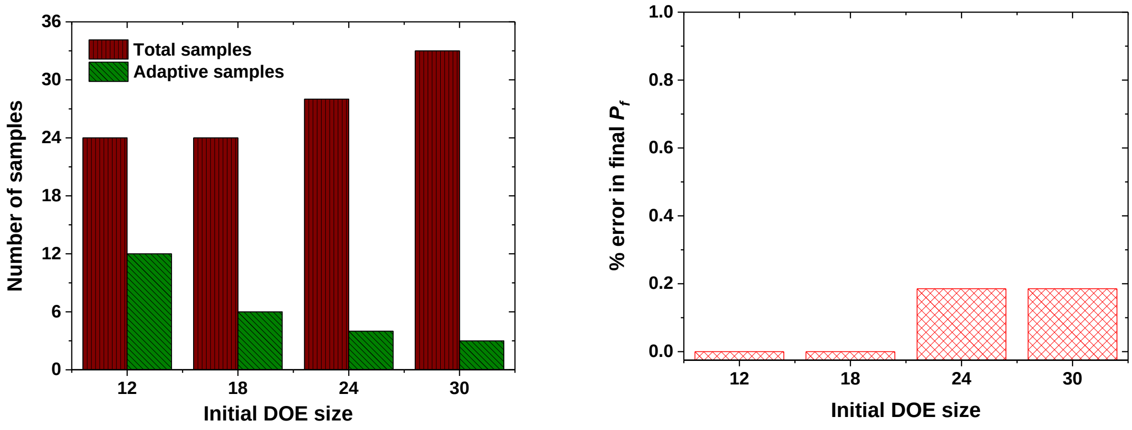

Figure 4. DOE sensitivity analysis by varying initial DOE size for the second LSF $g_1(x)$ (p_o = 5 N/mm^2; p_i = 1.05 N/mm^2; λ = 3).

The reliability study is now performed with respect to the second LSF $g_2(x)$ i.e. Eq. 4. The initial DOE is constructed according to the UD table $U_{12}(12^3)$. The values of P_f, N_E, N_{MC} and COV of P_f by the proposed adaptive Kriging, AK-MCS and direct MCS methods for varying p_o (p_i = 0.5 N/mm^2; ε = 0.02), varying p_i (p_o = 5 N/mm^2; ε = 0.02) and varying ε (p_o = 3.25 N/mm^2; p_i= 0.5 N/mm^2) are presented in Table 5, 6 and 7, respectively. The proposed adaptive Kriging approach is quite efficient as comparatively smaller number of samples (N_E) are required than the AK-MCS method. It is important to note that in three cases i.e. p_o = 2.75N/mm^2 of Table 5, p_i = 1.7 N/mm^2 of Table 6 and ε = 0.025 of Table 7, the AK-MCS method has failed to update the value of P_f as the U learning function based on the initial Kriging model of the AK-MCS method unable to detect any point within the MCS population even after the enrichment of the population up to one million samples. Also, no failure point is detected by the initial Kriging model of the AK-MCS method. However, there are actually adequate number of failure points to satisfy the acceptable COV of P_f. On the other hand, the proposed method does not suffer such a problem as the initial training samples are selected by UD.

Table 5. Comparison of P_f values for LSF $g_2(x)$ for varying p_o (p_i = 0.5 N/mm^2; ε = 0.02)

p_o (N/mm^2)	Direct MCS		AK-MCS		Proposed Adaptive Kriging	
	P_f (N_E)	N_{MC} (COV of P_f)	P_f (N_E)	N_{MC} (COV of P_f)	P_f (N_E)	N_{MC} (COV of P_f)
2.75	0.00127 (5×10^5)	5×10^5 (4.0%)	-	-	0.00126 (12+27)	3.5×10^5 (4.76%)
3	0.00400 (2×10^5)	2×10^5 (3.5%)	0.00405 (12+49)	1×10^5 (4.96%)	0.00402 (12+36)	1×10^5 (4.98%)
3.25	0.00890 (1×10^5)	1×10^5 (3.3%)	0.00890 (12+64)	1×10^5 (3.34%)	0.00890 (12+44)	1×10^5 (3.34%)
3.5	0.01937 (1×10^5)	1×10^5 (2.3%)	0.01938 (12+74)	1×10^5 (2.25%)	0.01937 (12+47)	1×10^5 (2.25%)
3.75	0.03860 (1×10^5)	1×10^5 (1.6%)	0.03974 (12+62)	1×10^5 (1.55%)	0.03976 (12+49)	1×10^5 (1.55%)

Table 6. Comparison of probability of failure P_f values for LSF $g_2(x)$ for varying p_i and (p_o = 5 N/mm^2; ε = 0.02)

p_i (N/mm^2)	Direct MCS		AK-MCS		Proposed Adaptive Kriging	
	P_f (N_E)	N_{MC} (COVof P_f)	P_f (N_E)	N_{MC} (COVof P_f)	P_f (N_E)	N_{MC} (COVof P_f)
1.3	0.00983 (1×10^5)	1×10^5 (3.2%)	0.00983 (12+42)	1×10^5 (3.17%)	0.00983 (12+40)	1×10^5 (3.17%)
1.4	0.00611 (1×10^5)	1×10^5 (4.0%)	0.00611 (12+54)	1×10^5 (4.03%)	0.00610 (12+40)	1×10^5 (4.04%)
1.5	0.00411 (1×10^5)	1×10^5 (4.9%)	0.00411 (12+59)	1×10^5 (4.92%)	0.00411 (12+32)	1×10^5 (4.92%)
1.6	0.00295 (2×10^5)	2×10^5 (4.1%)	0.00291 (12+49)	1.5×10^5 (4.78%)	0.00291 (12+37)	1.5×10^5 (4.78%)
1.7	0.00192 (3×10^5)	3×10^5 (4.2%)	-	-	0.00194 (12+30)	2.5×10^5 (4.54%)

Table 7. Comparison of probability of failure P_f values for LSF $g_1(x)$ for varying ε and (p_o = 3.25 N/mm^2; p_i= 0.5 N/mm^2)

ε	Direct MCS		AK-MCS		Proposed Adaptive Kriging	
	P_f (N_E)	N_{MC} (COVof P_f)	P_f (N_E)	N_{MC} (COVof P_f)	P_f (N_E)	N_{MC} (COVof P_f)
0.0175	0.01488 (1×10^5)	1×10^5 (2.6%)	0.01488 (12+52)	1×10^5 (2.57%)	0.01490 (12+43)	1×10^5 (2.57%)
0.02	0.00890 (1×10^5)	1×10^5 (3.3%)	0.00890 (12+64)	1×10^5 (3.34%)	0.00890 (12+44)	1×10^5 (3.34%)
0.0225	0.00540 (1×10^5)	1×10^5 (4.3%)	0.00539 (12+48)	1×10^5 (4.30%)	0.00532 (12+35)	1×10^5 (4.32%)
0.025	0.00406 (2.5×10^5)	2.5×10^5 (3.1%)	-	-	0.00393 (12+50)	1.5×10^5 (4.11%)
0.0275	0.00280 (2.5×10^5)	2.5×10^5 (3.8%)	0.00283 (12+75)	1.5×10^5 (4.85%)	0.00282 (12+35)	1.5×10^5 (4.86%)

The absolute percentage errors in estimating P_f values are presented in Fig. 5. The improved accuracy of the proposed adaptive Kriging method (error > 1% in only one case) is also observed to be better than the AK-MCS method (error > 1% in four cases).

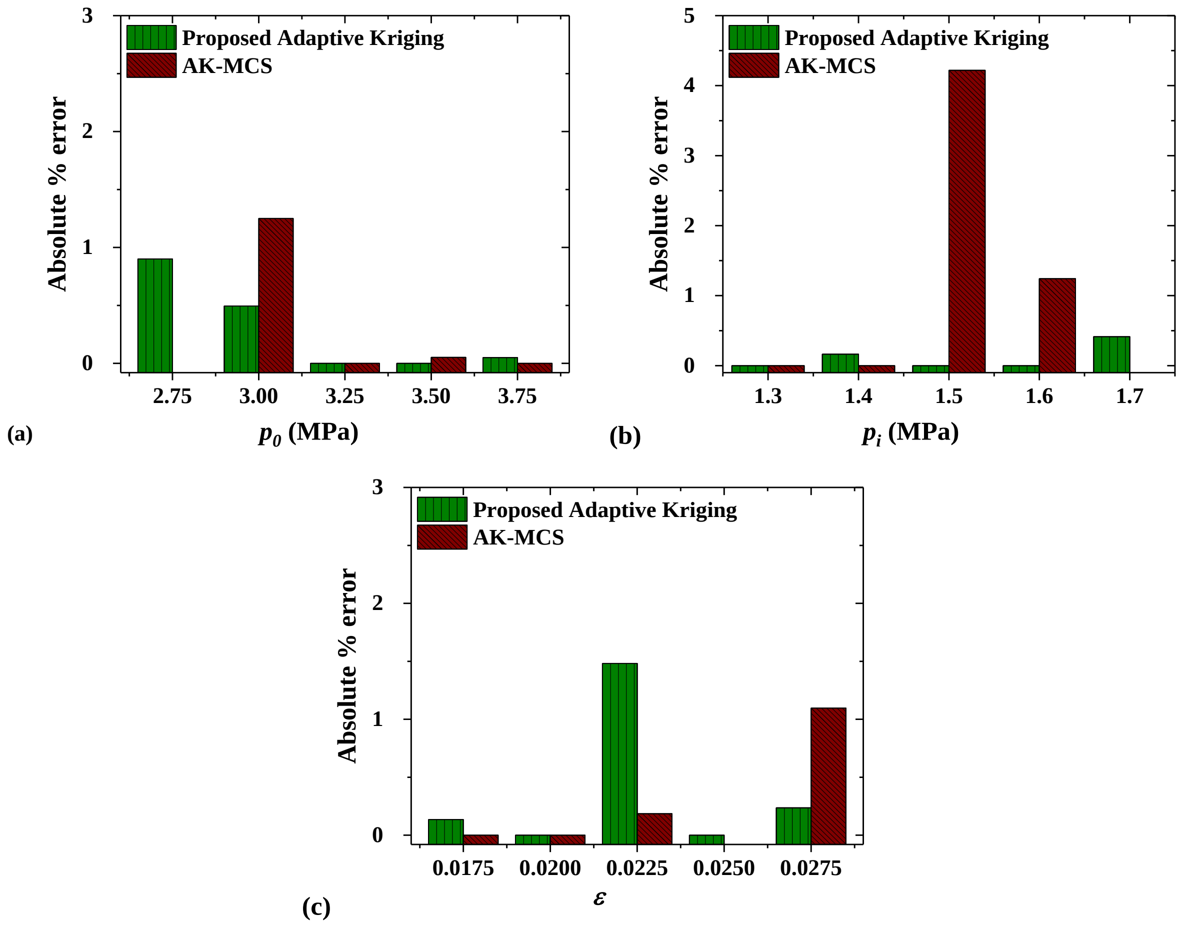

Fig. 5. Comparison of absolute percentage errors in estimating P_f values by the proposed adaptive Kriging and the AK-MCS methods for the second LSF $g_2(x)$ of Example 1.

Like the first LSF, the DOE sensitivity study for the second LSF is also performed by varying the initial DOE size. For p_o = 2.75 N/mm^2, p_i = 0.5 N/mm^2 and ε = 0.02, the P_f values are estimated by the proposed method by starting with four different initials DOEs according to UD tables $U_{12}(12^3)$, $U_{18}(18^3)$, $U_{24}(24^3)$ and U_{30} (30^3). The numbers of training samples required by four different cases are shown in Fig. 6 (a) and the associated absolute percentage errors are presented in Fig. 6 (b). The number of adaptive samples are varying (27 to 37) depending upon the initial DOE size. However, in all the four cases, the absolute errors in estimating the failure probability are less than 2.5% indicating the robustness of the proposed approach.

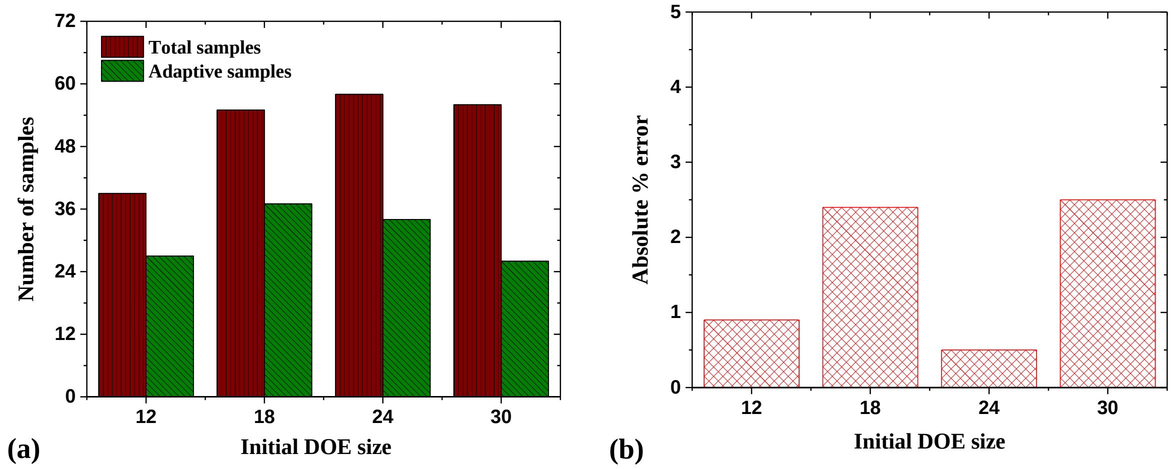

Fig. 6. DOE sensitivity analysis for varying initial DOE size for g_2x (p_o = 2.75 N/mm^2; p_i = 0.5 N/mm^2; ε = 0.02).

Further, DOE sensitivity study is performed by varying the arrangement of the UD table $U_{12}(12^3)$ for constructing the initial DOE. In this regard, it can be noted that users can assign one column of UD table to any of the random variables. Thus, a number of permutations are possible to construct the DOE according to a unique UD table. For p_o = 2.75 N/mm^2; p_i = 0.5 N/mm^{2}and ε = 0.02, five such different DOE arrangements are taken as the initial DOE for estimating P_f by the proposed approach. The numbers of adaptive training samples required by five different cases are shown in Fig. 7 (a). Fig. 7 (b) shows the absolute percentage errors for the five cases. It is observed that the different initial DOEs consisting of different samples requires varying number of adaptive samples subsequently different number of total samples. However, the P_f values estimated by the present approach are quite accurate (error < 2.5%) in all the five cases. This clearly shows the robustness of the proposed approach.

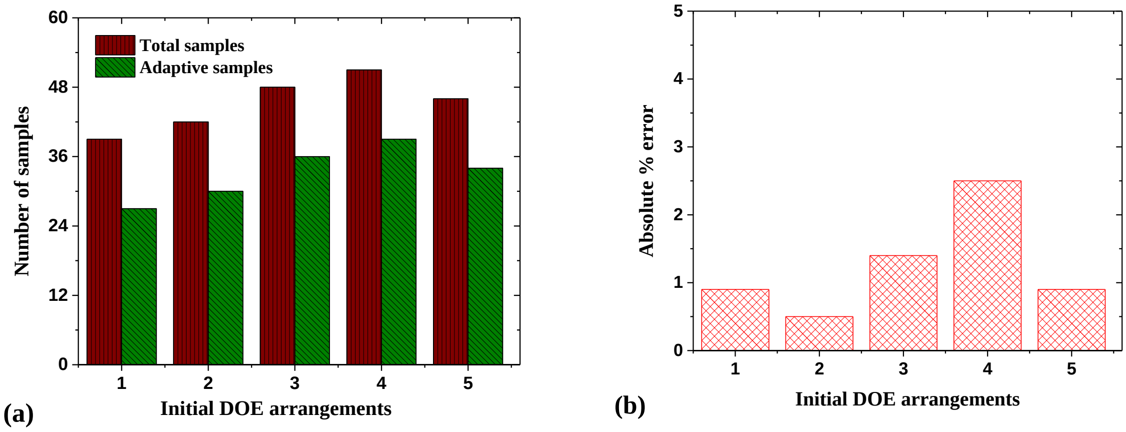

Fig. 7. DOE sensitivity analysis results for varying arrangements of the UD table $U_{12}(12^3)$ to construct the initial DOE for the second limit state function (p_o = 2.75 N/mm^2; p_i = 0.5 N/mm^2; ε = 0.02).

3.2 Example 2: a real-life tunnel

The next example is a highway tunnel involving implicit LSF. It is basically a 3.245 km long highway tunnel of radius 5.9 m with a maximum cover of 350 m, reinforced with concrete liner and rock bolt. A diagrammatic representation of the tunnel is shown in Fig. 4. The problem is taken from Su et al. [61] where the reliability analysis involving implicit LSF have been conducted. The safety assessment is performed based on the assumptions that the tunnel is in an axisymmetric condition. The rock mass is homogeneous, isotropic and follows the Mohr-Coulomb failure criterion. The more details on this may be seen in [61]. The installation of the rock bolt in the rock modifies the mechanical properties of the rock mass. The improvement is simulated by the modified cohesion given by [62]: $c'=c+\tau_b A_b/(S_c S_l)$, which is to be applied while calculating the support pressure, $P_{i,bolt}$.

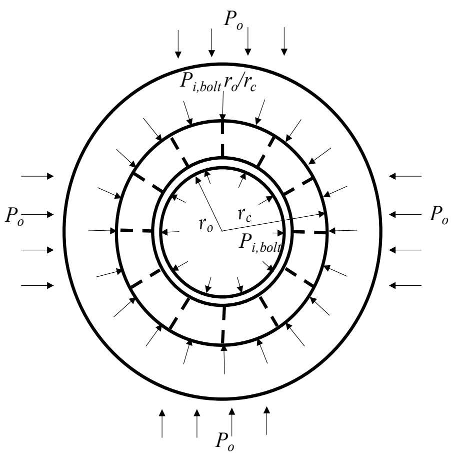

Fig. 8. Tunnel configuration under the axisymmetric geometric condition (redrawn from Su et al. [61])

The LSF is based on the failure of the primary support. The failure is considered to occur when the rock pressure $P_{i,min}$ exceeds the support pressure, i.e. the combined support pressure in shotcrete and rock bolts ($P_{i,shot}$ and $P_{i,bolt}$). The related derivations of expression of $P_{i,shot}$, $P_{i,bolt}$ and $P_{i,rock}$ may be seen in Su et al. [61]. For brevity, the expressions are directly used here to describe the LSF. The derivation of the LSF is presented in detail in Su et al. [61]. The LSF is represented as,

$$g(x) = (P_{i,shot} + P_{i,bolt}) - P_{i,\mathbf{min}} \qquad (8)$$

Where:

$$P_{i,\min} = \gamma r_o \left\{ \left[\frac{(1-\sin\varphi)(c\cot\varphi + P_o)}{(1+\sin\varphi)(c\cot\varphi + P_{i,\min})} \right]^{\frac{1-\sin\varphi}{2\sin\varphi}} - 1 \right\} \tag{9}$$

$$P_{i,shot} = K_s \left(u_{r_o} - u_o \right) \Big/ r_o \tag{10}$$

$$P_{i,bolt} = \frac{\left[(u_{r_o} - u_o^a) - (u_{r_c} - u_o^a \frac{r_o}{r_c}) \right] E_b A_b}{(r_c - r_o) S_c S_l} \tag{11}$$

$$K_s = E_s d \,/ \left[r_o (1 - \nu_s^2) \right]$$

$$u_r = \frac{r_o^2 (1+\nu)(P_o \sin\varphi + c\cos\varphi)}{Er} \times \left[\frac{(1-\sin\varphi)(c\cot\varphi + P_o)}{c\cot\varphi + P_{i,\min}} \right]^{\frac{1-\sin\varphi}{\sin\varphi}} \tag{12}$$

The various parameters involved in the above equations are defined in table 8. It may be noted that the equation of $P_{i,min}$ is implicit in nature which brings complexity to the analysis process. The value of $P_{i,min}$ is obtained by an iterative process where a value of $P_{i,min}$ is assumed to initiate the iteration. The iteration is continued till the value of $Pi_{,min}$ converges.

Table 8 Details of the various parameters of the tunnel

Parameter	Description	Parameter	Description
C	Cohesion	*d*	Thickness of the concrete liner
Γ	Unit weight	K_s	Stiffness modulus of the concrete liner
φ	Angle of internal friction	A_b	Cross-sectional area of rockbolt
E	Modulus of elasticity of rockmass	S_l and S_c.	Longitudinal and circumferential spacing of rockbolts
N	Poisson's ratio of rockmass	$E_{b.}$	The Young's modulus of the bolt material
E_s	Elastic modulus of shotcrete	v_s	Poisson's ratio of shotcrete
r_o	Radius of tunnel	*L*	Length of rockbolt
Rc	r_o+*L*	P_o	Hydrostatic far field pressure
u_o	Initial tunnel closure before installation of lining	u_o^a	Radial displacement of the tunnel wall post-installation of rock bolt
u_{ro}	Radial displacement at r_o	u_{rc},	Radial displacement at r_c

The parameters *c*, *φ*, P_o, *E*, u_o and *d* are considered as random in the reliability analysis; the statistical properties of which are shown in Table 8. The rest of the values are considered having the values: r_o=

(11.8/2) m = 5.9 m, u_o^a=1:92 cm, γ = 26.5 kN/m^3, ν = 0.5, E_s = 28 GPa, ν_s = 0.167, E_b= 210 GPa, L = 3.0 m, A_b = 380.13 mm^2, τ_b= 312 MPa, and S_c = S_l = 1.0 m.

Table 9 Statistical proeprties of the random parameters [61]

Parameters (unit)	Distribution	Mean	SD	Truncation Limit	
				Lower	Upper
c (MPa)	Truncated Normal	0.5070	0.0675	0.3045	0.7095
φ (º)	Truncated Normal	28.7000	2.3000	21.8000	35.6000
p_o(MPa)	Truncated Normal	9.9750	0.7110	7.8420	12.1080
E (GPa)	Truncated Normal	4.3700	0.5244	2.7968	5.9432
u_o (mm)	Truncated Normal	32	4	20	44
d (mm)	Truncated Normal	203	20	143	263

The P_f values are obtained by varying the mean values of P_o in the first parametric study and by varying the mean values of u_o in the second. The SD for u_o and P_o are taken as 12.5% and 7.125% of the considered mean values, respectively for the two parametric studies. The experimental domains for these two random variables are within range of mean ± 3×SD. Like the previous example, the initial DOE for each case is constructed according to the UD table U12(126). The values of P_f, N_E, N_{MC} and COV of P_f obtained by the proposed adaptive Kriging approach, AK-MCS and direct MCS methods are shown in Table 10 and 11 for varying P_o and u_o, respectively. The proposed adaptive Kriging method requires a smaller number of samples than the AK-MCS method in most of the cases.

Table 10. Comparison of probability of failure P_f values for LSF $g_3(x)$ for varying p_o

Mean of p_o (N/mm^2)	Direct MCS		AK-MCS		Proposed Adaptive Kriging	
	P_f (N_E)	N_{MC} (COV of P_f)	P_f (N_E)	N_{MC} (COVof P_f)	P_f (N_E)	N_{MC} (COVof P_f)
9.5	0.01050 (1×10^5)	1×10^5 (3.07%)	0.01050 (12+114)	1×10^5 (3.07%)	0.01036 (12+112)	1×10^5 (3.09%)
9.75	0.00606 (1×10^5)	1×10^5 (4.05%)	0.00606 (12+97)	1×10^5 (4.05%)	0.00605 (12+98)	1×10^5 (4.05%)
10	0.00405 (1.5×10^5)	1.5×10^5 (4.86%)	0.00383 (12+78)	1.1×10^5 (4.86%)	0.003809 (12+75)	1.1×10^5 (4.88%)
10.25	0.00202 (2×10^5)	2×10^5 (4.97%)	0.00202 (12+105)	2×10^5 (4.97%)	0.00202 (12+94)	2×10^5 (4.97%)
10.5	0.00124 (3.5×10^5)	3.5×10^5 (4.80%)	0.00124 (12+104)	3.5×10^5 (4.80%)	0.001237 (12+108)	3.5×10^5 (4.80%)

Table 11. Comparison of probability of failure P_f values for LSF $g_3(x)$ for varying u_o

Mean of u_o(mm)	Direct MCS		AK-MCS		Proposed Adaptive Kriging	
	P_f (N_E)	N_{MC} (COV of P_f)	P_f (N_E)	N_{MC} (COVof P_f)	P_f (N_E)	N_{MC} (COVof P_f)
30	0.00166 (2.5×10^5)	2.5×10^5 (4.9%)	0.01050 (12+96)	2.5×10^5 (4.90%)	0.01036 (12+84)	2.5×10^5 (4.92%)
31	0.00255 (2×10^5)	2×10^5 (4.4%)	0.00606 (12+84)	1.4×10^5 (4.93%)	0.00605 (12+86)	1.5×10^5 (4.75%)
32	0.00391 (1.5×10^5)	1.5×10^5 (4.1%)	0.00383 (12+111)	1.1×10^5 (4.81%)	0.003809 (12+94)	1.1×10^5 (4.82%)
33	0.00548 (1×10^5)	1×10^5 (4.3%)	0.00202 (12+88)	1×10^5 (4.26%)	0.00202 (12+84)	1×10^5 (4.26%)
34	0.00811 (1×10^5)	1×10^5 (3.5%)	0.00124 (12+83)	1×10^5 (3.5%)	0.001237 (12+83)	1×10^5 (3.5%)

The absolute percentage errors in estimated failure are shown in the Fig. 9. The proposed adaptive Kriging method is found to be quite efficient and accurate enough for this six-dimensional complex tunnel reliability analysis problem with implicit LSF.

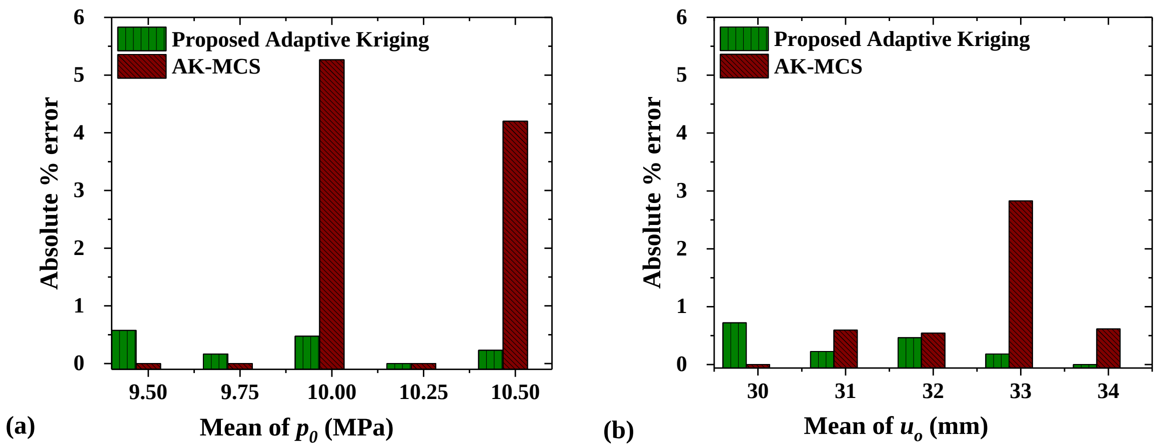

Fig. 9. Comparison of absolute percentage errors in estimating P_f values by the proposed adaptive Kriging and the AK-MCS methods for Example 2.

Like the previous example, two DOE sensitivity studies are further performed. In the first study, the P_f values are obtained by the proposed approach considering the distribution of random variables as per Table 9 for the four different initials DOEs according to UD tables $U_{12}(12^6)$, $U_{18}(18^6)$, $U_{24}(24^6)$ and U_{30} (30^6). The number of training samples required by the proposed approach for different cases are shown in Fig. 10 (a). Number of adaptive samples for different cases are varying from 81 to 87 and the total number of actual function evaluations is in the range of 99 to 111. The absolute error in estimating the failure probability is very less for all the cases as may be seen from Fig. 10 (b).

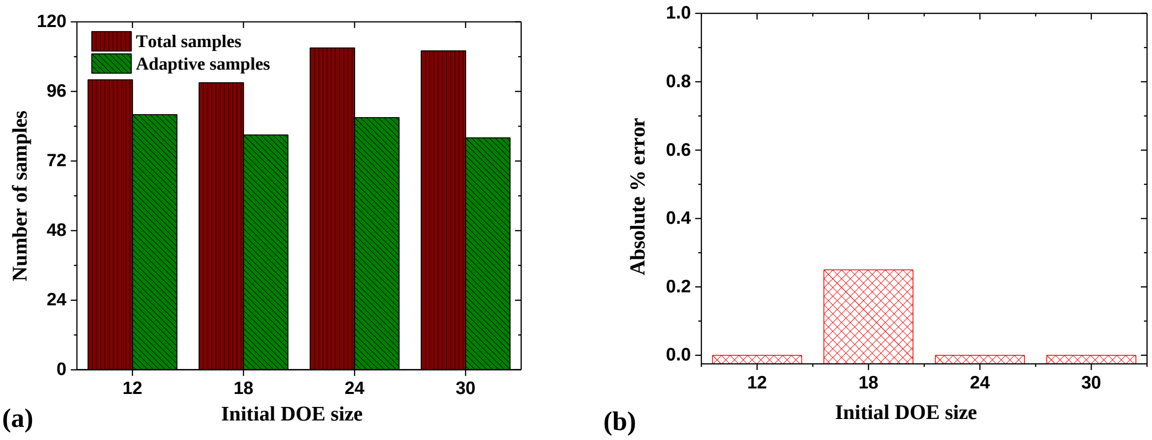

Fig. 10. DOE sensitivity analysis by varying the initial DOE size for example 2.

The second DOE sensitivity analysis is performed by varying the arrangement of the UD table $U_{12}(12^6)$ for constructing the initial DOE. In doing so, six different permutation of column numbers are taken to construct the six different initial DOE. The number of training samples required and absolute errors in estimating failure probability are depicted in Figs. 11 (a) and (b), respectively. It can be observed that approximately same number of adaptive samples (86 to 91) are required by the proposed method to get a close estimate (deviation < 2.5%) of P_f values for all the six cases. The results of the sensitivity study of this example also clearly established the robustness of the proposed approach.

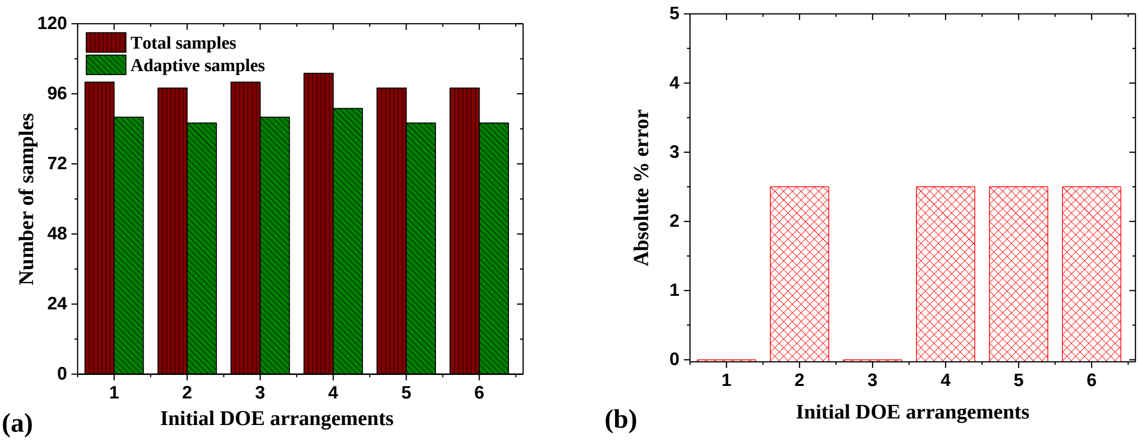

Fig. 11. DOE sensitivity analysis by varying arrangements of the UD table $U_{12}(12^3)$ to construct the initial DOE for example 2.

3.3 Example 3: a tunnel reliability problem involving FE analysis with geostatic stress field

A circular tunnel reinforced with concrete liner and rock bolt is considered as the last example for demonstrating the effectiveness of the proposed adaptive Kriging approach of reliability analysis of realistic tunnel analysis problem involving FE analysis with geostatic stress field. The tunnel is 5m in radius and is at a depth of 400m. The structural analysis model is prepared using ABAQUS software. The rockmass is modelled as a plain strain homogeneous section having overall dimension of 60m wide by 430m deep. The FE model consists of 824 number of 8-node plane strain quadrilateral (CPE8R: 8-node biquadratic plane strain quadrilateral) element, with 2599 number of nodes as shown in Fig. 12. The Mohr-Coulomb (c-ϕ) failure criterion is used to define the elasto-plastic behaviour of the rock mass. The bottom edge is fixed, and the side edges are supported by roller supports, restricting the translation in horizontal direction. The concrete liner is elastic in nature and is modelled as 80 numbers of homogeneous beam element (B21: 2-node linear beam in a plane). A total of 24 rock bolts of 5m length are provided at a uniform circumferential spacing of 1.3m, and the bolt is modelled as homogeneous elastic bar element (T2D2: 2-node linear 2-D truss). Each rockbolt is composed of 10 number of elements with 11number of nodes. The structural analysis is performed using ABAQUS software. The stress analysis of the tunnel is conducted by geostatic field-based FE method with the density of the rock mass as given in Table 12. The more details of the application of the geostatic field-based FE analysis can be seen elsewhere [63–65]. The process of defining the geostatic stress field may be also seen in the ABAQUS software manual available at https://abaqus-docs.mit.edu. The excavation is simulated by stiffness reduction technique, in which the elastic modulus of the rock mass within the tunnel expected to be excavated is reduced to 2% of the initial elastic modulus. The properties involving concrete and steel are deterministic in nature and is enlisted in Table 12. The elastic modulus, cohesion and angle of internal friction of the rock mass are considered random. The statistical information of these parameters is presented in the Table 13.

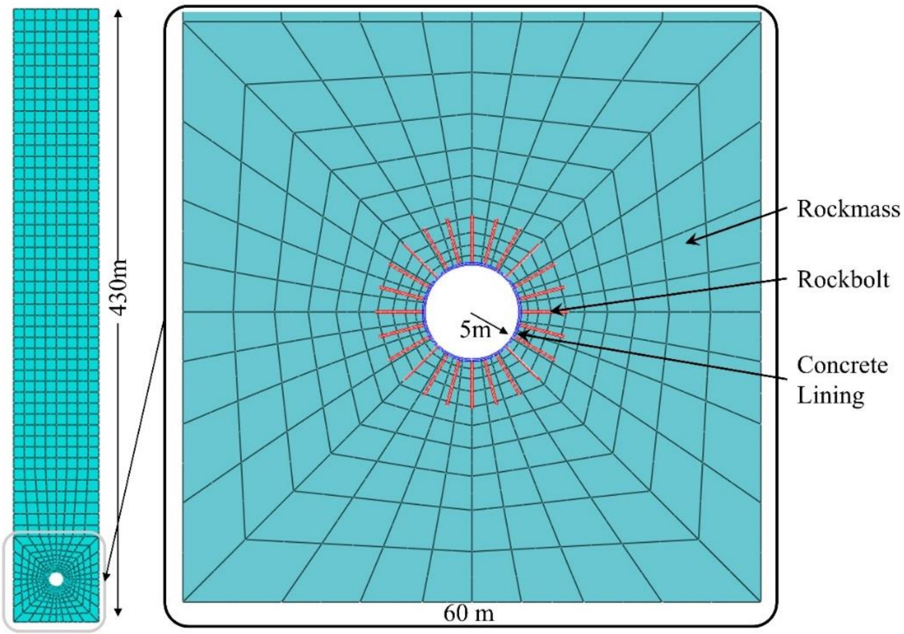

Fig. 12. Finite Element mesh of the numerical model of the tunnel showing the lining and rockbolts

Table 12. Variou parameters of the tunnel model

		Model Parameter
Rock Mass:		
	Density	m= 2.5485×10^{-9} tonne/mm^3
	Elastic Modulus	E_r= 12000 MPa
	Poisson's Ratio	v_r = 0.22
	Cohesion	c = 1.2 MPa
	Frictional Angle	φ = 42°
Concrete Lining:		
	Tunnel Radius	R_t = 5.0 m
	Elastic Modulus	E_c = 28000 MPa
	Poisson's Ratio	v_c =0.27
Rock Bolt:		
	Elastic Modulus	E_b = 210000 MPa
	Poisson's Ratio	v_b = 0.30
	Nos. of Bolt	N_b = 24 Nos
	Length	L_b = 5 m
	Diameter	D_b = 25mm
	Spacing	S_b = 1.3m

Table 13. Statistical properties of the considered random variables

Properties	Distribution	Mean	SD	Truncated Limit	
				Lower	Upper
E_{RM} (N/mm^2)	Truncated Normal	12000	1000	9000	15000
c (N/mm^2)	Truncated Normal	1.2	0.1	0.8	1.6
Φ (degree)	Truncated Normal	42	3	35	49

The reliability analysis is performed with respect to the radial closure of the tunnel wall [60]. The limit state equation is defined as follows:

$$g(x) = u_{\max} - u_{actual} \tag{13}$$

In Eq. (13), u_{actual} is the value of the maximum radial displacement at the tunnel wall and u_{max} is its allowable value, taken as 10mm [49].

The initial DOE is constructed using 12 number of samples selected according to the UD table $U_{12}(12^3)$. The tunnel reliability is estimated for varying thickness of the tunnel. The number of samples considered for the direct MCS technique is ten thousand. The values of P_f, N_E, N_{MC} and COV of P_f obtained by the proposed adaptive Kriging, AK-MCS and direct MCS methods are shown in Table 14 for three different concrete lining thickness. The value of u_{max} is taken as 10mm [49]. In Table 14, the COV of P_f for the direct MCS technique is seen to be very high as limited number of simulations is considered in the direct MCS method. It can be noted that each simulation on a CPU with AMD Ryzen 5-4600H 3.00 GHz processor and 16 GB RAM takes 14 s. Hence, the time required for ten thousand simulations is 39 h. Due to time constraint, the number of samples taken in the direct MCS method for each case is limited to 10^4 samples. An importance sampling method is further employed as a variance reduction technique to estimate the P_f values using actual LSF for consistent comparative study. In doing so, a most probable failure point (MPFP) is first obtained by FORM, and then, 1000 importance samples are generated by shifting the input space to the MPFP. The results of the importance sampling method, denoted as FORM + IS, is also presented in Table 14. For the proposed Kriging method and the AK-MCS method, the initial N_{MC} value is taken as 10^5, and the incremental value of 5×10^4 sample is taken if COV of P_f is higher than 5%. It can be seen from Table 14 that the efficiency of the proposed method is better than the AK-MCS method in most of instances with respect to the total number of function evaluation (N_E). This reveals the effectiveness of the proposed Kriging method in reliability analysis of tunnel involving FE analysis considering realistic geostatic stress field.

Table 14 Comparison of probability of failure P_f values for LSF $g_4(x)$ for varying Concrete lining thickness, t

t (mm)	FORM + IS		Direct MCS		AK-MCS		Proposed Adaptive Kriging	
	P_f (N_E)	N_{MC} (COV of P_f)	P_f (N_E)	N_{MC} (COV of P_f)	P_f (N_E)	N_{MC} (COV of P_f)	P_f (N_E)	N_{MC} (COV of P_f)
300	0.00234 (21+1000)	1×10^3 (6.54%)	0.00246 (1×10^4)	1×10^4 (20%)	0.00251 (12+15)	1.6×10^5 (4.98%)	0.00251 (12+14)	1.6×10^5 (4.98%)
325	0.00112 (21+1000)	1×10^3 (8.29%)	0.0012 (1×10^4)	1×10^4 (29%)	0.00119 (12+17)	4×10^5 (4.58%)	0.00120 (12+15)	3.4×10^5 (4.94%)
350	0.00279 (21+1000)	1×10^3 (14.77%)	0.0003 (1×10^4)	1×10^4 (58%)	0.00030 (12+17)	1.34×10^6 (4.96%)	0.00030 (12+17)	1.34×10^6 (4.96%)

Further, the P_f values are estimated by the proposed adaptive Kriging for the tunnel with 300 mm concrete line thickness for varying u_{max} from 9.75 mm to 10.25 mm. The number of adaptive samples required, and the total number of training samples are shown in Fig. 13 (a). The P_f values are estimated by the proposed adaptive Kriging, the direct MCS and FORM + IS and are presented in Fig. 13 (b). The estimates of the P_f values by the proposed adaptive Kriging approach are very close to that of obtained by the direct MCS and FORM + IS indicating the efficiency of the proposed method.

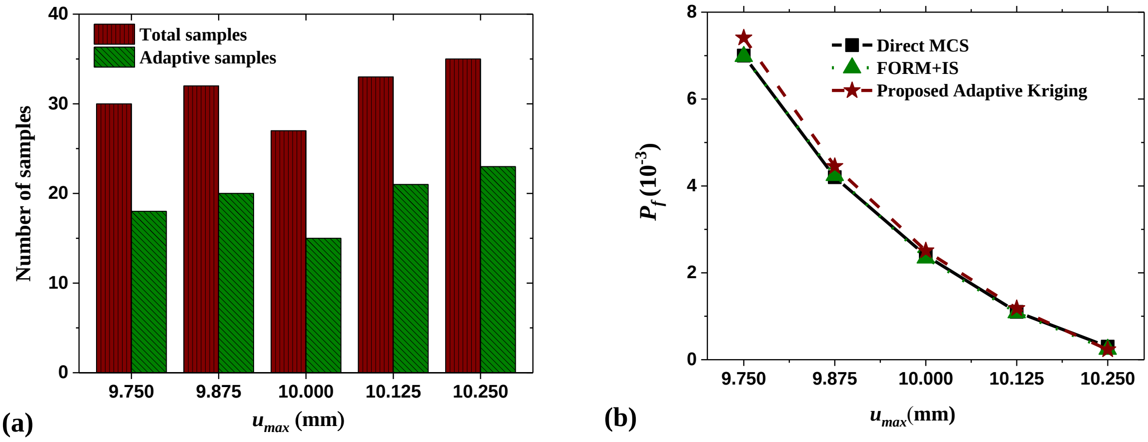

Fig. 13 Parametice study for the tunnel with 300 mm concrete line thickness by varying u_{max}.

Like the previous examples, two DOE sensitivity studies are also performed for the present example. In doing so, the P_f values are further obtained by the proposed approach with 300 mm concrete line thickness and u_{max} = 10 mm by varying initial DOE size. Four different initials DOEs are constructed according to UD tables $U_{12}(12^3)$, $U_{18}(18^3)$, $U_{24}(24^3)$ and U_{30} (30^3). The number of training samples required by the proposed approach for different cases are shown in Fig. 14 (a). The number of adaptive samples requirement is decreasing with the increase in the size of the initial DOE. The estimated failure probabilities for all the cases are shown in Fig. 10 (b) and the values are observed to be very close to each other indicating the robustness of the proposed approach.

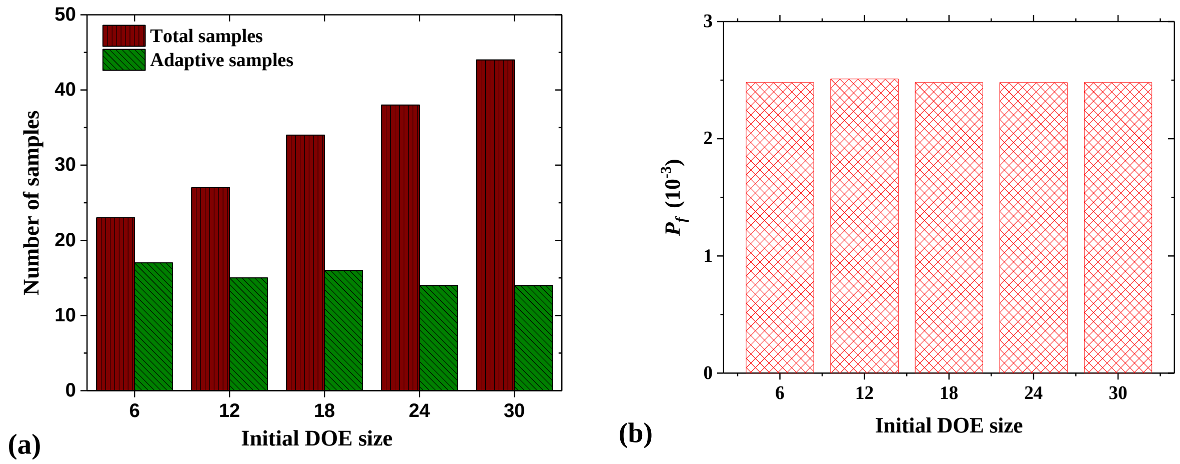

Fig. 14. DOE sensitivity analysis by varying initial DOE size for the tunnel with 300 mm concrete line thickness and u_{max} = 10 mm.

Another DOE sensitivity analysis is performed by varying the arrangement of UD table $U_{12}(12^3)$ to construct the initial DOE for the tunnel with 350 mm concrete line thickness and u_{max} = 10 mm. The number of adaptive samples are presented in Fig. 15 (a) and are ranging from 19 to 24 for six different cases. The P_f values for different cases are shown in Fig. 15 (b) and are found to be very close to each other. The results reveal the robustness of the proposed approach.

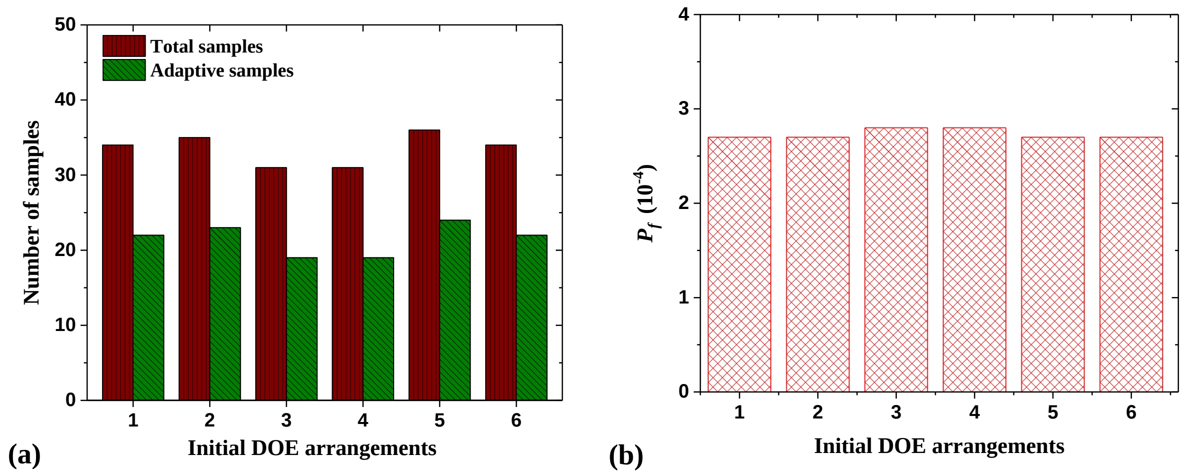

Fig. 15. DOE sensitivity analysis by varying arrangement of UD table $U_{12}(12^3)$ to construct the initial DOE for the tunnel with 350 mm concrete line thickness and u_{max} = 10 mm.

4. Summary and conclusion

An efficient adaptive Kriging based MCS method to improve the Kriging prediction by sequentially selecting training points based on the joint PDF of the involved random parameters is explored for reliability analysis of underground tunnels. Three tunnel reliability analysis examples are studied to demonstrate the effectiveness of the proposed approach. The performance is compared with the AK-MCS method in terms of accuracy and computational demand. The accuracy is judged with reference to the direct MCS technique, and, the total number of actual function evaluations is considered for comparing the computational demand. In most of the cases, the proposed method is noted to be superior to the AK-MCS method for all the three tunnel examples studied here. In all cases, the accuracy of the proposed method is quite high (absolute error in estimating failure probability is less than 1% in most of the cases). Further, DOE sensitivity analyses of the proposed method are performed for each example by varying the initial DOE size and also by varying the arrangements of columns of the UD table according to which the initial DOE is build. The results of the sensitivity study of all the three example problems in general show the robustness of the proposed approach. The proposed approach is generic in nature and can be applied using any other metamodels for reliability analysis.

References

[1] E. Hoek, Reliability of Hoek-Brown estimates of rock mass properties and their impact on design, International Journal of Rock Mechanics and Mining Sciences. 35 (1998) 63–68. https://doi.org/https://doi.org/10.1016/S0148-9062(97)00314-8.

[2] J. Hadjigeorgiou, J.P. Harrison, Uncertainty and sources of error in rock engineering, in: Harmonising Rock Engineering and the Environment - Proceedings of the 12th ISRM International Congress on Rock Mechanics, 2012. https://doi.org/10.1201/b11646-393.

[3] O. Ditlevsen, H.O. Madsen, Structural Reliability Methods, Wiley, 2005. https://books.google.co.in/books/about/Structural_Reliability_Methods.html?id=E5ibQgAACAAJ&source=kp_book_description&redir_esc=y (accessed June 10, 2019).

[4] S.-Kyum. Choi, R. v. Grandhi, R.A. Canfield, Reliability-based structural design, Springer, 2007.

[5] R. Teixeira, M. Nogal, A. O’Connor, Adaptive approaches in metamodel-based reliability analysis: A review, Structural Safety. 89 (2021) 102019. https://doi.org/10.1016/J.STRUSAFE.2020.102019.

[6] C.G. Bucher, U. Bourgund, A fast and efficient response surface approach for structural reliability problems, Structural Safety. 7 (1990) 57–66. https://doi.org/10.1016/0167-4730(90)90012-E.

[7] I. Kaymaz, Application of kriging method to structural reliability problems, Structural Safety. 27 (2005) 133–151. https://www.sciencedirect.com/science/article/pii/S0167473004000463 (accessed June 10, 2019).

[8] A. Roy, R. Manna, S. Chakraborty, Support vector regression based metamodeling for structural reliability analysis, Probabilistic Engineering Mechanics. 55 (2019) 78–89. https://doi.org/10.1016/J.PROBENGMECH.2018.11.001.

[9] J. Deng, Structural reliability analysis for implicit performance function using radial basis function network, International Journal of Solids and Structures. 43 (2006) 3255–3291. https://doi.org/10.1016/J.IJSOLSTR.2005.05.055.

[10] M. Papadrakakis, V. Papadopoulos, N.D. Lagaros, Structural reliability analyis of elastic-plastic structures using neural networks and Monte Carlo simulation, Comput. Methods Appl. Mech. Engrg. 136 (1996) 145–163.

[11] R. Rackwitz, B. Fiessler, Structural reliability under combined random load sequences, Computers and Structures. 9 (1978) 489–494. https://doi.org/10.1016/0045-7949(78)90046-9.

[12] A. der Kiureghian, M. de Stefano, Efficient Algorithm for Second-Order Reliability Analysis, Journal of Engineering Mechanics. 117 (1991). https://doi.org/10.1061/(asce)0733-9399(1991)117:12(2904).

[13] Y.-G. Zhao, T. Ono, A general procedure for first/second-order reliabilitymethod (FORM/SORM), Structural Safety. 21 (1999) 95–112. https://doi.org/10.1016/S0167-4730(99)00008-9.

[14] L. Faravelli, Response-Surface Approach for Reliability Analysis, Journal of Engineering Mechanics. 115 (1989) 2763–2781. https://doi.org/10.1061/(ASCE)0733-9399(1989)115:12(2763).

[15] J.R. Gaxiola-Camacho, H. Azizsoltani, F.J. Villegas-Mercado, A. Haldar, A novel reliability technique for implementation of Performance-Based Seismic Design of structures, Engineering Structures. 142 (2017) 137–147. https://doi.org/10.1016/J.ENGSTRUCT.2017.03.076.

[16] C. Kim, S. Wang, K.K. Choi, Efficient Response Surface Modeling by Using Moving Least-Squares Method and Sensitivity, AIAA Journal. 43 (2005) 2404–2411. https://doi.org/10.2514/1.12366.

[17] H.S. Li, Z. Lü, Z.F. Yue, Z.Z. Lu, Z.F. Yue, Support vector machine for structural reliability analysis, Applied Mathematics and Mechanics (English Edition). 27 (2006) 1295–1303. https://doi.org/10.1007/s10483-006-1001-z.

[18] C.M. Rocco, J.A. Moreno, Fast Monte Carlo reliability evaluation using support vector machine, Reliability Engineering and System Safety. 76 (2002) 237–243. https://doi.org/10.1016/S0951-8320(02)00015-7.

[19] B. Richard, C. Cremona, L. Adelaide, A response surface method based on support vector machines trained with an adaptive experimental design, Structural Safety. 39 (2012) 14–21. https://doi.org/10.1016/j.strusafe.2012.05.001 (accessed June 10, 2019).

[20] H. Dai, H. Zhang, W. Wang, G. Xue, Structural Reliability Assessment by Local Approximation of Limit State Functions Using Adaptive Markov Chain Simulation and Support Vector Regression, Computer-Aided Civil and Infrastructure Engineering. 27 (2012) 676–686. https://doi.org/10.1111/j.1467-8667.2012.00767.x.

[21] A. Hosni Elhewy, E. Mesbahi, Y. Pu, Reliability analysis of structures using neural network method, Probabilistic Engineering Mechanics. 21 (2006) 44–53. https://doi.org/https://doi.org/10.1016/j.probengmech.2005.07.002.

[22] M.R. Rajashekhar, B.R. Ellingwood, A new look at the response surface approach for reliability analysis, Structural Safety. 12 (1993) 205–220. https://doi.org/10.1016/0167-4730(93)90003-J.

[23] S. Goswami, S. Ghosh, S. Chakraborty, Reliability analysis of structures by iterative improved response surface method, Structural Safety. 60 (2016) 56–66. https://doi.org/10.1016/J.STRUSAFE.2016.02.002.

[24] R. Farag, A. Haldar, A novel reliability evaluation method for large engineering systems, Ain Shams Engineering Journal. 7 (2016) 613–625. https://doi.org/10.1016/J.ASEJ.2016.01.007.

[25] N. Roussouly, F. Petitjean, M. Salaun, A new adaptive response surface method for reliability analysis, Probabilistic Engineering Mechanics. 32 (2013) 103–115. https://www.sciencedirect.com/science/article/pii/S0266892012000525.

[26] B. Echard, N. Gayton, M. Lemaire, AK-MCS: An active learning reliability method combining Kriging and Monte Carlo Simulation, Structural Safety. 33 (2011) 145–154. https://www.sciencedirect.com/science/article/pii/S0167473011000038.

[27] B. Echard, N. Gayton, M. Lemaire, N. Relun, A combined Importance Sampling and Kriging reliability method for small failure probabilities with time-demanding numerical models, Reliability Engineering and System Safety. 111 (2013) 232–240. https://doi.org/10.1016/j.ress.2012.10.008.

[28] Q. Pan, D. Dias, An efficient reliability method combining adaptive Support Vector Machine and Monte Carlo Simulation, Structural Safety. 67 (2017) 85–95. https://doi.org/10.1016/j.strusafe.2017.04.006.

[29] N.C. Xiao, M.J. Zuo, C. Zhou, A new adaptive sequential sampling method to construct surrogate models for efficient reliability analysis, Reliability Engineering and System Safety. 169 (2018) 330–338. https://doi.org/10.1016/j.ress.2017.09.008.

[30] N.C. Xiao, M.J. Zuo, W. Guo, Efficient reliability analysis based on adaptive sequential sampling design and cross-validation, Applied Mathematical Modelling. 58 (2018) 404–420. https://doi.org/10.1016/j.apm.2018.02.012.

[31] Z. Sun, J. Wang, R. Li, C. Tong, LIF: A new Kriging based learning function and its application to structural reliability analysis, Reliability Engineering and System Safety. 157 (2017) 152–165. https://doi.org/10.1016/j.ress.2016.09.003.
[32] X. Huang, J. Chen, H. Zhu, Assessing small failure probabilities by AK-SS: An active learning method combining Kriging and Subset Simulation, Structural Safety. 59 (2016) 86–95. https://doi.org/10.1016/j.strusafe.2015.12.003.
[33] C. Xu, W. Chen, J. Ma, Y. Shi, S. Lu, AK-MSS: An adaptation of the AK-MCS method for small failure probabilities, Structural Safety. 86 (2020) 101971. https://doi.org/10.1016/j.strusafe.2020.101971.
[34] W. Yun, Z. Lu, X. Jiang, L. Zhang, P. He, AK-ARBIS: An improved AK-MCS based on the adaptive radial-based importance sampling for small failure probability, Structural Safety. 82 (2020) 101891. https://doi.org/10.1016/j.strusafe.2019.101891.
[35] N. Lelièvre, P. Beaurepaire, C. Mattrand, N. Gayton, AK-MCSi: A Kriging-based method to deal with small failure probabilities and time-consuming models, Structural Safety. 73 (2018) 1–11. https://doi.org/10.1016/j.strusafe.2018.01.002.
[36] S. Kabasi, A. Roy, S. Chakraborty, Reliability analysis of structures by iterative sequential sampling based response surface, Proceedings of the Institution of Civil Engineers - Structures and Buildings. (2021) 1–10. https://doi.org/10.1680/jstbu.20.00220.
[37] A. Roy, S. Chakraborty, Reliability analysis of structures by a three-stage sequential sampling based adaptive support vector regression model, Reliability Engineering & System Safety. 219 (2022) 108260. https://doi.org/10.1016/J.RESS.2021.108260.
[38] A. Roy, S. Chakraborty, Support vector regression based metamodel by sequential adaptive sampling for reliability analysis of structures, Reliability Engineering and System Safety. 200 (2020) 106948. https://doi.org/10.1016/j.ress.2020.106948.
[39] P. Oreste, A probabilistic design approach for tunnel supports, Computers and Geotechnics. 32 (2005). https://doi.org/10.1016/j.compgeo.2005.09.003.
[40] H.Z. Li, B.K. Low, Reliability analysis of circular tunnel under hydrostatic stress field, Computers and Geotechnics. 37 (2010) 50–58. https://doi.org/10.1016/j.compgeo.2009.07.005.
[41] G. Chen, G. Su, T. Li, New method of reliability analysis for deep tunnel, Applied Mechanics and Materials. 50–51 (2011) 864–868. https://doi.org/10.4028/www.scientific.net/AMM.50-51.864.
[42] G. Mollon, D. Dias, A.H. Soubra, Probabilistic analysis of the face stability of circular tunnels, Geotechnical Special Publication. (2009) 348–355. https://doi.org/10.1061/41022(336)45.
[43] Q. Lü, B.K. Low, Probabilistic analysis of underground rock excavations using response surface method and SORM, Computers and Geotechnics. 38 (2011) 1008–1021. https://doi.org/10.1016/j.compgeo.2011.07.003.

[44] Q. Lü, H.Y. Sun, B.K. Low, Reliability analysis of ground-support interaction in circular tunnels using the response surface method, International Journal of Rock Mechanics and Mining Sciences. 48 (2011) 1329–1343. https://doi.org/10.1016/j.ijrmms.2011.09.020.

[45] W. Zhang, A.T.C. Goh, Reliability assessment on ultimate and serviceability limit states and determination of critical factor of safety for underground rock caverns, Tunnelling and Underground Space Technology. 32 (2012) 221–230. https://doi.org/10.1016/j.tust.2012.07.002.

[46] Q. Lü, C.L. Chan, B.K. Low, Probabilistic evaluation of ground-support interaction for deep rock excavation using artificial neural network and uniform design, Tunnelling and Underground Space Technology. 32 (2012) 1–18. https://doi.org/10.1016/j.tust.2012.04.014.

[47] H. Liu, B.K. Low, System reliability analysis of tunnels reinforced by rockbolts, Tunnelling and Underground Space Technology. (2017). https://doi.org/10.1016/j.tust.2017.03.003.

[48] H. Zhao, Z. Ru, X. Chang, S. Yin, S. Li, Reliability analysis of tunnel using least square support vector machine, Tunnelling and Underground Space Technology. 41 (2014) 14–23. https://doi.org/10.1016/j.tust.2013.11.004.

[49] Q. Wang, H. Fang, L. Shen, Reliability analysis of tunnels using a metamodeling technique based on augmented radial basis functions, Tunnelling and Underground Space Technology. 56 (2016) 45–53. https://doi.org/10.1016/j.tust.2016.02.007.

[50] Q. Wang, H. Fang, Reliability analysis of tunnels using an adaptive RBF and a first-order reliability method, Computers and Geotechnics. 98 (2018) 144–152. https://doi.org/10.1016/j.compgeo.2018.02.011.

[51] S. Chakraborty, D. Majumder, Hybrid reliability analysis framework for reliability analysis of tunnels, Journal of Computing in Civil Engineering. (2018). https://doi.org/10.1061/(ASCE)CP.1943-5487.0000759.

[52] D. Majumder, S. Chakraborty, R. Chowdhury, Probabilistic analysis of tunnels: A hybrid polynomial correlated function expansion based approach, Tunnelling and Underground Space Technology. (2017). https://doi.org/10.1016/j.tust.2017.07.009.

[53] T.Z. Li, X.L. Yang, An efficient uniform design for Kriging-based response surface method and its application, Computers and Geotechnics. 109 (2019) 12–22. https://doi.org/10.1016/j.compgeo.2019.01.009.

[54] J. Sacks, S.B. Schiller, W.J. Welch, Designs for computer experiments, Technometrics. 31 (1989) 41–47. https://doi.org/10.1080/00401706.1989.10488474.

[55] I. Kaymaz, Application of kriging method to structural reliability problems, Structural Safety. 27 (2005) 133–151. https://doi.org/https://doi.org/10.1016/j.strusafe.2004.09.001.

[56] T.J. Santner, B.J. Williams, W.I. Notz, Space-Filling Designs for Computer Experiments, in: Springer, New York, NY, 2003: pp. 121–161. https://doi.org/10.1007/978-1-4757-3799-8_5.

[57] K.-T. Fang, D.K.J. Lin, P. Winker, Y. Zhang, Uniform Design: Theory and Application, Technometrics. 42 (2000) 237–248. https://doi.org/10.1080/00401706.2000.10486045.

[58] S.N. Lophaven, H.B. Nielsen, J. Søndergaard, H.B. Nielsen, DACE — A Matlab Kriging Toolbox (Version 2.0), IMM Informatiocs and Mathematical Modelling. (2002).

[59] Duncan Fama, Numerical modeling of yield zones in weak rock, Pergamon Press Ltd., Oxford (United Kingdom), United Kingdom, 1993. https://doi.org/https://doi.org/.

[60] W.Z. Chen, G.J. Wu, S.P. Jia, The application of ABAQUS in tunnel and underground engineering, Beijing: Water Conservancy and Hydropower Press. (2010).

[61] Y.H. Su, X. Li, Z.Y. Xie, Probabilistic evaluation for the implicit limit-state function of stability of a highway tunnel in China, Tunnelling and Underground Space Technology. 26 (2011) 422–434. https://doi.org/10.1016/j.tust.2010.11.009.

[62] P.P. Oreste, Analysis of structural interaction in tunnels using the covergence-confinement approach, Tunnelling and Underground Space Technology. 18 (2003) 347–363. https://doi.org/10.1016/S0886-7798(03)00004-X.

[63] R. Dai, Z.F. Li, J. Wang, Research on initial geo-stress balance method based on abaqus, Journal of Chongqing Technology and Business University (Natural Science Edition). 29 (2012) 76–81.

[64] X.U. Lei, A general method for the accurate equilibrium of complex initial in-situ stress field, Journal of China Three Gorges University: Natural Science Edition. 34 (2012) 30–33.

[65] X.Y. Wang, Y.L. Yuan, C.M. Hu, Y. Mei, Research on the Geostatic Stress Field Procedure under Complex Conditions, Advances in Civil Engineering. 2021 (2021). https://doi.org/10.1155/2021/6674369.